



## EWSR1-SMAD3 positive fibroblastic tumor

Lu Zhao<sup>a,b</sup>, Meng Sun<sup>a,b</sup>, I. Weng Lao<sup>a,b</sup>, Lin Yu<sup>a,b</sup>, Jian Wang<sup>a,b,\*</sup>

<sup>a</sup> Department of Pathology, Fudan University Shanghai Cancer Center, Shanghai, China

<sup>b</sup> Department of Oncology, Shanghai Medical College, Fudan University, Shanghai, China

### ARTICLE INFO

#### Keywords:

Fibroblastic tumor  
Fluorescence in situ hybridization  
Next-generation sequencing  
EWSR1-SMAD3

### ABSTRACT

We present a case of *EWSR1-SMAD3* positive fibroblastic tumor that occurred in a 24-year-old man who presented with a recurrent tumor in the dorsum of his right foot. Magnetic resonance imaging (MRI) demonstrated a subcutaneous nodule located in the third metatarsophalangeal joint region, measuring  $10 \times 8 \times 5$  mm in size. Histological examination revealed a monomorphic spindle cell tumor composed of cellular fascicles of bland fibroblasts with hyalinization. Immunohistochemically, the tumor showed diffuse nuclear staining of ERG. Fluorescence in situ hybridization (FISH) assessment demonstrated an unbalanced rearrangement of the *EWSR1* gene. Further next-generation sequencing (NGS) analysis identified *EWSR1-SMAD3* gene fusion. Molecular detection may be helpful for identifying new entities, in particular to those that lack lineage-specific differentiation by conventional pathological examinations.

### 1. Introduction

With the advances in molecular genetics, especially the application of next-generation sequencing (NGS) in routine clinical practice, more and more soft tissue tumors have been found to harbor novel recurrent gene fusions and emerge as new entities (Miettinen et al., 2019). In this study, we present a case of spindle cell tumor that occurred in the right foot dorsum of a 24-year-old man. Although the tumor has unique clinicopathological features, it is difficult to categorize in the current classification systems of soft tissue tumors. Next-generation sequencing (NGS) identified the *EWSR1-SMAD3* fusion gene, consistent with the recently described *EWSR1-SMAD3* positive fibroblastic tumor, a provisional novel entity (Kao et al., 2018; Michal et al., 2018). With the ability to identify new fusion genes and their chimeric transcripts, molecular detection has been playing an increasingly important role in the diagnosis and refined classification of soft tissue tumors.

#### 1.1. Brief report

The patient was a 24-year-old man who presented with pain on the right forefoot for a period of three months. He had surgery in a local hospital two years ago, with excision of a neoplasm diagnosed originally as 'giant cell tumor of the tendon sheath, diffuse-type'. Physical examination revealed ill-defined subcutaneous nodules on the dorsum of the right foot which were thought as recurrent. Ultrasound discovered two adjacent hypoechoic nodules in the subcutis. Magnetic

resonance imaging (MRI) examination showed that the nodules were located in the third metatarsophalangeal joint region, with a low signal on T1WI and a high signal on T2WI (Fig. 1). Laboratory examinations were all within normal ranges. Re-excision of the recurrent lesion was carried out in the local hospital. The pathological diagnosis this time was 'a spindle cell neoplasm of intermediate or low-grade malignancy, with low grade malignant peripheral nerve sheath tumor (MPNST) not excluded'. For further medical attention, the pathological materials were referred to our department for consultation.

#### 1.2. Histology

Grossly, the specimen of the primary tumor and the recurrent tumor consisted of pieces of fibroadipose tissue measuring  $1.3 \times 0.6 \times 0.3$  cm and  $3.5 \times 2 \times 1$  cm in aggregate, respectively. On cut section, the solid components were gray with firm consistency.

Microscopically, both tumors were located in the subcutis and displayed a nodular or plexiform growth pattern (Fig. 2A, B). They were ill-circumscribed, showing infiltration into the adipose tissue (Fig. 2C). The primary tumor was composed of cellular fascicles of monomorphic bland spindle cells, which had elongated nuclei with finely dispersed chromatin and small inconspicuous nucleoli with the absence of mitotic activity (Fig. 2D). In some areas, there was prominent stromal hyalinization (Fig. 2E). Focal stippled calcification was also present (Fig. 2F). The recurrent tumor exhibited similar features. There was a vague zonation pattern with central hypocellular hyalinization and the

\* Corresponding author at: Department of Pathology, Fudan University Shanghai Cancer Center, 270 Dong An Street, Shanghai 200032, China.

E-mail address: [softtissuetumor@163.com](mailto:softtissuetumor@163.com) (J. Wang).

<https://doi.org/10.1016/j.yexmp.2019.104291>

Received 19 June 2019; Received in revised form 5 July 2019; Accepted 30 July 2019

Available online 31 July 2019

0014-4800/© 2019 Elsevier Inc. All rights reserved.

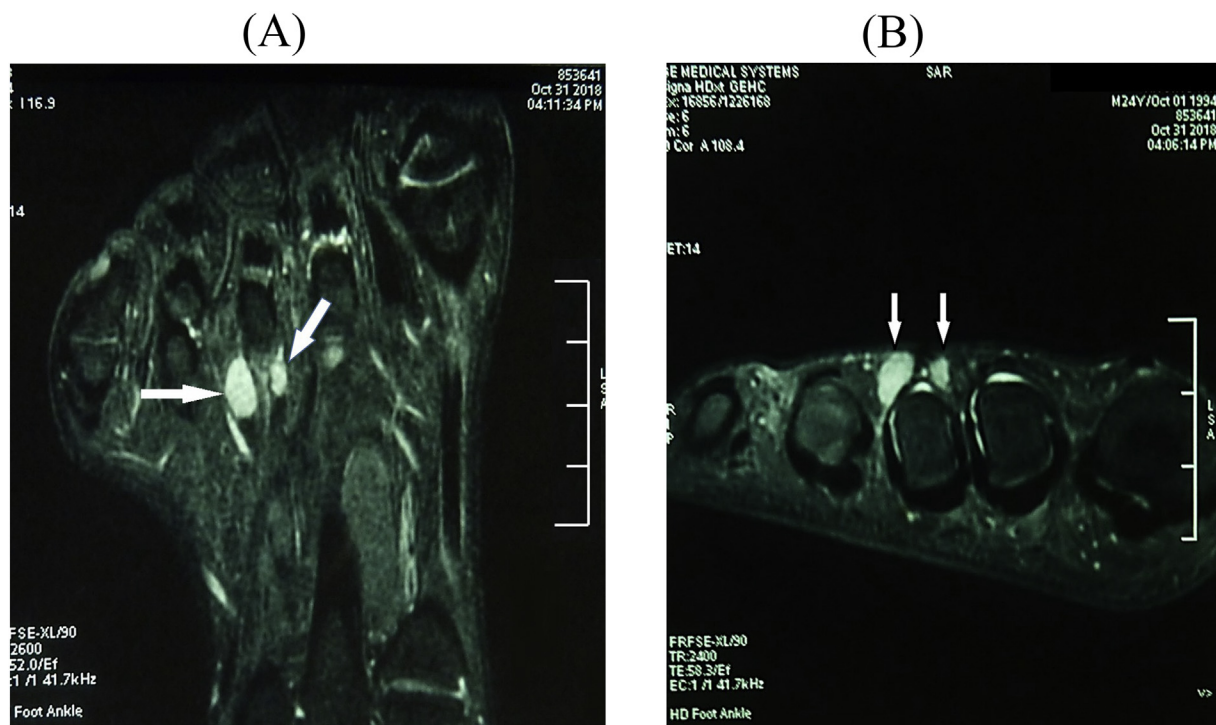


**Fig. 1.** Radiological features. The sagittal (A) and coronal (B) plain MRI of the right foot revealed two small nodules with a high signal on T2WI, which were located at the third metatarsophalangeal joint region.

hypercellular component at the periphery (Fig. 2F). The stroma also showed myxoid change, alternating with the hyalinized components (Fig. 2G).

### 1.3. Immunohistochemistry

Immunohistochemical study was performed on 4- $\mu$ m thick unstained sections generated from formalin-fixed paraffin-embedded (FFPE) blocks on Ventana Automated Immunostainer (BenchMarker Ultra, Ventana Medical System, Inc.) according to the manufacturer's manual. A wide panel of antibodies were used, including pancytokeratin (AE1/AE3, 1:50; Dako), epithelial membrane antigen (EMA) (E29, 1:200; Dako), bcl-2 (clone 124, 1:100; Dako), CD99 (12E7, 1:100; Dako), vimentin (V9, 1:100; Dako), CD34 (QBEnd 10, 1:100; Dako),  $\alpha$ -smooth muscle actin ( $\alpha$ -SMA) (1A4, 1:200; Dako), desmin (clone D33, 1:250; Dako),  $\beta$ -catenin (polyclonal, 1:600, Mindray), S100 protein (polyclonal, 1:2500; Dako), SOX10 (SDM2, ready to use; Celeris Diagnostics), H3K27Me3 (RM175, 1:2000, Remab), MUC4 (8G7, 1:100; Abcam), ERG (EPR3864, prediluted; Roche), CD31 (JC70A, 1:100; Dako), SATB2 (SATBA4B10, 1:100, ZSGB) and Ki67 (MIB1, 1:150; Dako). Appropriate positive and negative controls were run concurrently with all antibodies tested.

By immunohistochemistry, the spindle cells in both primary and recurrent tumors showed diffuse and strong nuclear staining for ERG (Fig. 3A). Focal and weak expression of SATB2 was noted in the recurrent tumor (Fig. 3B). Ki67 index in both tumors was low (< 2%). Other antibodies used in the study all yielded negative results.

### 1.4. Molecular genetic studies

#### 1.4.1. Fluorescence in situ hybridization

Interphase fluorescence in situ hybridization (FISH) study was carried out on 5- $\mu$ m thick sections generated from FFPE tissues for assessment of the *EWSR1* gene rearrangement. Briefly, the sections were incubated in a humidified chamber (HYBrite™ system; Vysis, Abbott, Des Plaines, IL) using dual color break-apart probes of *EWSR1* (22q12)

(HYBrite™ system; Vysis, Abbott, Des Plaines, IL) according to the manufacturer's protocol. The fluorescence signals were analyzed using an Olympus BX51 fluorescence microscope (Olympus, Tokyo, Japan). A total of 200 successive nuclei were assessed. The cutoff level for score as positive was when at least 20% of the nuclei showed a break-apart signal and/or loss of telomeric part.

FISH assay showed an unbalanced rearrangement of *EWSR1* with loss of the telomeric part in both primary and recurrent tumors (Fig. 4A).

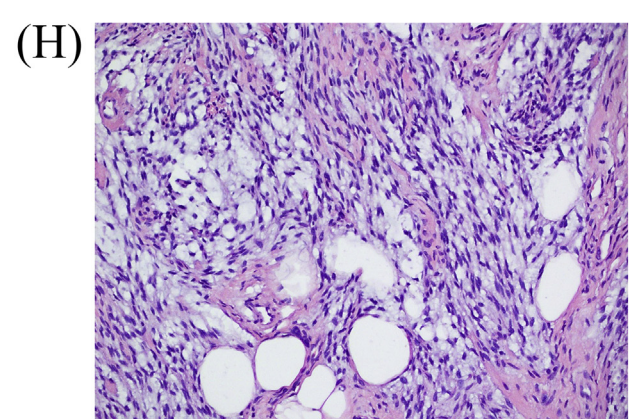
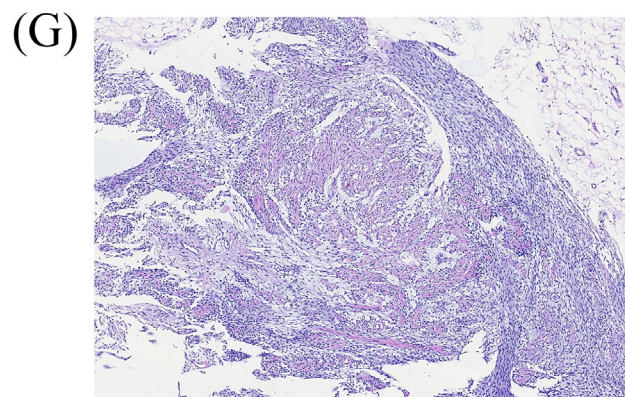
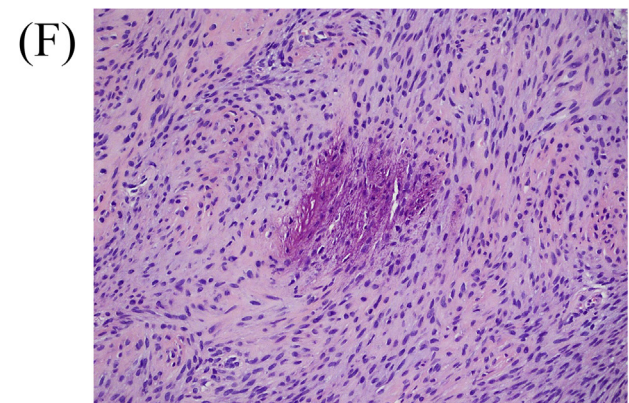
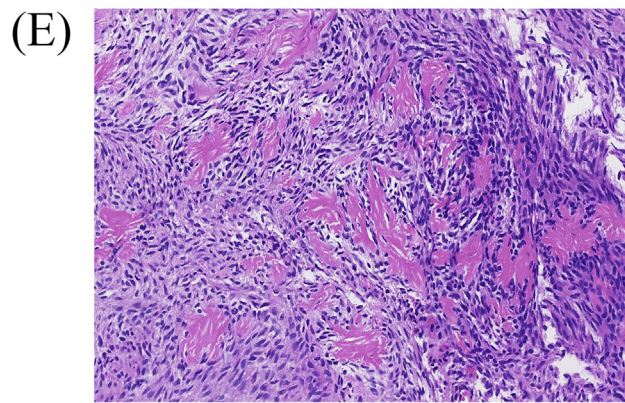
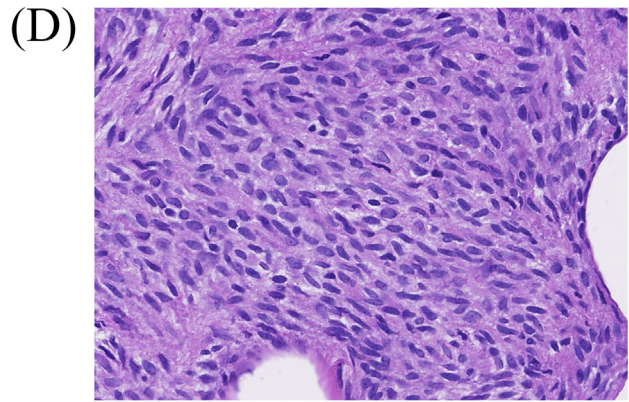
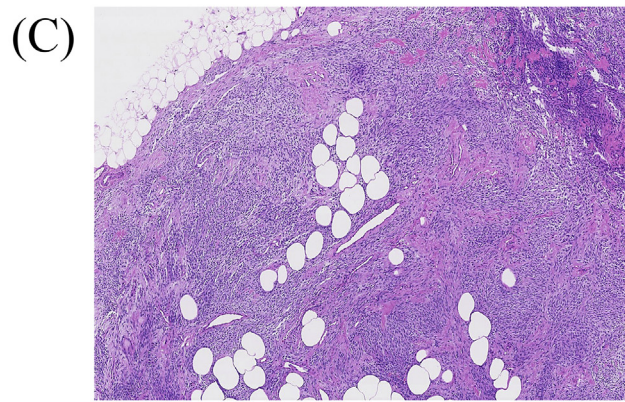
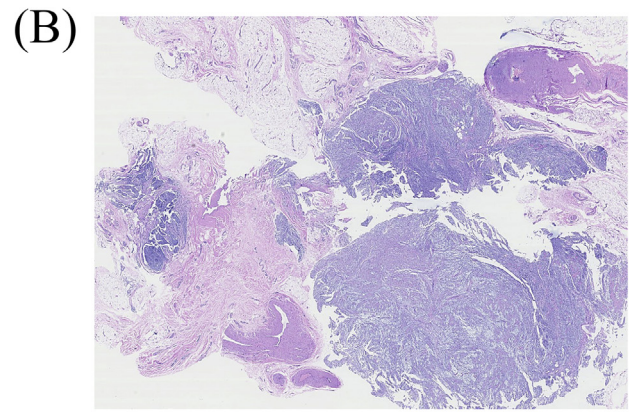
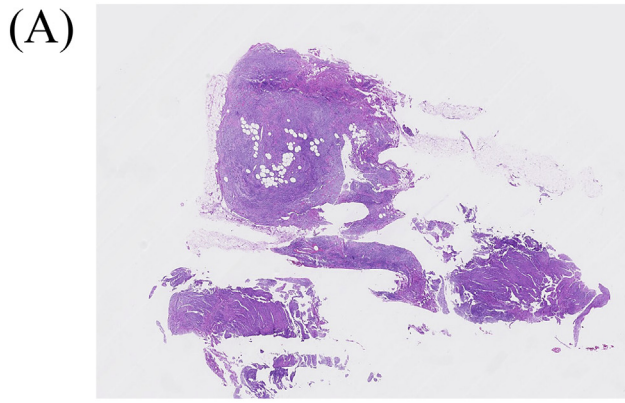
#### 1.4.2. Identification of *EWSR1*-*SMAD3* fusion by NGS

To identify the fusion candidate, FFPE samples from the primary tumor were used. A minimum of 15 unstained slides was obtained. RNA was extracted followed by cDNA synthesis. Genetic profiling was analyzed by 578 genes based (DNA) and 544 genes based (RNA) panel sequencing on an Illumina platform. All steps were performed according to the manufacturer's instruction.

By NGS analysis, *EWSR1* exon7-*SMAD3* exon 6 fusion was identified as a result of t(15;22)(q22;q12) (Fig. 4B). In addition, the amplification of the collagen type 1 alpha 1 (*COL1A1*), calreticulin (*CALR*), the cyclin-dependent kinase 4 (*CDK4*), tetraspanin 31 (*TSPAN31*, also referred as SAS), and the signal transducer and activator of transcription 6 (*STAT6*) were detected. The tumor mutational burden was relatively low (1.8 Muts/Mb).

## 2. Discussion

Soft tissue tumors comprise a large heterogeneous group of entities. Genetically, many of them are characterized by chromosomal rearrangements resulting in recurrent gene fusions, which can be used as molecular diagnostic markers. Well-known gene fusions include the *SS18-SSX1/2* fusion resulting from t(X;18) translocation in synovial sarcoma, and *EWSR1-FLI1* or *ERG* fusion resulting from t(11;22) or t(21;22) in Ewing sarcoma. To detect tumor-specific gene fusions in examined cases, interphase FISH using commercial probes or reverse-transcription polymerase chain reaction (RT-PCR) with specifically



(caption on next page)

**Fig. 2.** Microscopic features. A. The primary tumor was located in the subcutis and had a nodular growth pattern. (H&E, original magnification, scanning view). B. Tumorous nodules in the recurrent tumor (H&E, original magnification, scanning view). C. Tumor cells infiltrated into the adipose tissue. (H&E, original magnification,  $\times 100$ ). D. Cellular fascicles of bland spindle cells. (H&E, original magnification,  $\times 400$ ). E. Prominent stromal hyalinization. (H&E, original magnification,  $\times 200$ ). F. Focal stippled calcification. (H&E, original magnification,  $\times 200$ ). G. A vague zonation pattern with central hypocellular hyalinization and peripheral hypercellular areas. (H&E, original magnification,  $\times 40$ ). H. Alternating hyalinized and myxoid components. (H&E, original magnification,  $\times 200$ ).

designed primers has been widely used. However, these molecular techniques are considered unsuitable for tumors with unknown genetic abnormalities. Recently, the advent of NGS has provided a new strategy in the search for novel gene fusions (Groisberg et al., 2017). With the application of NGS in clinical practice, an increasing number of tumors have been identified as novel entities (Pierron et al., 2012; Choi et al., 2013; Agaram et al., 2016). In this study, we described a case of *EWSR1-SMAD3* positive fibroblastic tumor, a provisional new entity that has a predilection for the acral soft tissue. The novel *EWSR1-SMAD3* fusion gene was initially detected in an index case which occurred in the foot of a 1-year-old infant, presenting with an ill-defined dermal and subcutaneous nodule (Kao et al., 2018). Together with two additional cases showing similar histologic features and harboring identical gene fusion, the authors described a small series of *EWSR1-SMAD3* positive acral spindle cell neoplasm. An additional four cases were reported shortly after by another group of pathologists (Michal et al., 2018). Including the current case, there are eight cases of *EWSR1-SMAD3* positive fibroblastic tumor to date. In summary, the patient's age at presentation ranged from 1 to 68 years (mean, 36 years; median, 36.6 years) (Table 1). There was a female predominance with a ratio of 3:1. Except for one case affecting the calf, all the other 7 cases were located at the acral sites, including foot ( $n = 3$ ), heel ( $n = 1$ ), toe ( $n = 1$ ), hand ( $n = 1$ ) and thumb ( $n = 1$ ). Of note, one case each was located at the interphalangeal joint (case #2 of Michal et al.'s report) and metatarsophalangeal joint (current case) respectively. Clinically, all tumors presented as a dermal or subcutaneous nodule or mass ranging in size from 1 to 2 cm (mean, 1.3 cm; median, 1.2 cm). Because of locally infiltrative growth, 4 of 6 patients (67%) experienced local recurrence, mostly due to incomplete excision. The recurrence interval ranged from 5 months to 10 years, indicating that a long-term follow-up is warranted.

Histologically, *EWSR1-SMAD3* positive fibroblastic tumor was composed of uniform fibroblastic spindle cells that lack nuclear atypia, pleomorphism, prominent nucleoli, and mitotic activity. In adult cases, a distinctive zonation pattern with acellular central hyalinization and peripheral areas of cellular spindle cell fascicles was present. Stippled dystrophic calcification was found in one report case (case #2 of Kao et al.'s report) and in the current case. In addition, our case also showed alternative myxoid change of the stroma, which may have some vague resemblance to a low-grade MPNST.

Immunohistochemically, except for the equivocal weak staining of

keratin and EMA in one reported case (case #2 of Kao et al.'s report), the tumor is consistently negative for  $\alpha$ -SMA, CD34, S100 protein and SOX10. Interestingly, all eight cases showed diffuse ERG nuclear expression. However, our case demonstrated the absence of CD31 reactivity, denied the endothelial differentiation of neoplastic cells. The ubiquitous staining of ERG in the tumor is considered to attribute to the overexpression of ERG, revealed by RNA sequencing in the index case, as well as significant upregulation of FN1 mRNA expression, similar to other fibroblastic tumors.

*SMAD3*, one member of SMAD family (Flanders, 2004), contains the N-terminal Mad homology 1 (MH1), the C-terminal MH2 domains and a linker region connecting MH domains and plays as a signal transducer or transcriptional modulator in the transforming growth factor-beta (TGF- $\beta$ )/SMAD signal pathway (Zawel et al., 1998). Previous studies suggested that *SMAD3* was a key intracellular mediator in the regulation of cell proliferation, differentiation, and apoptosis, the production of extracellular matrix (ECM), the epithelial-mesenchymal transition (EMT), and the fibrosis mediated by TGF- $\beta$  (Kolossova et al., 2011; Ooshima et al., 2019). Besides *EWSR1-SMAD3* fusion, the *COL1A1* gene and *STAT6* gene were amplified in the current case. The former, one of the *SMAD3* targets, encodes the pro-alpha1 chains of type I collagen, abundant in bone, dermis, and tendon, and the later could be activated by interleukin-4 (IL-4) and binds to and activate collagen promoter in the lung fibrosis (Verrecchia et al., 2001; Buttner et al., 2004). These molecular genetic events closely interrelated with the fibrosis and the production of collagen, supporting a fibroblastic differentiation which was presumed through the whole transcriptome sequencing (Kao et al., 2018). Furthermore, the number of *CDK4*, *TSPAN31*, and *CALR* gene copies was detected to be increased in our case. There was growing evidence that *CDK4/CDK2* could phosphorylate *SMAD3* which would inhibit its transcriptional activity and give rise to tumorigenesis (Matsuura et al., 2004; Liu, 2006). *CALR* encoding a Ca<sup>2+</sup>-binding protein located in the endoplasmic reticulum, was mutated in some patients with myeloproliferative neoplasms (MPNs), however, its role in tumorigenesis remained unclear (Houen, 2019).

Regarding the tumor site as well as the histomorphology, the differential diagnoses in the current case embrace a variety of mesenchymal tumors, including spindle cell synovial sarcoma, calcifying aponeurotic fibroma, *NTRK* rearranged spindle cell mesenchymal tumor, low-grade MPNST and phosphaturic mesenchymal tumor. Spindle cell synovial sarcoma typically occurs in the deep soft tissue of extremities,

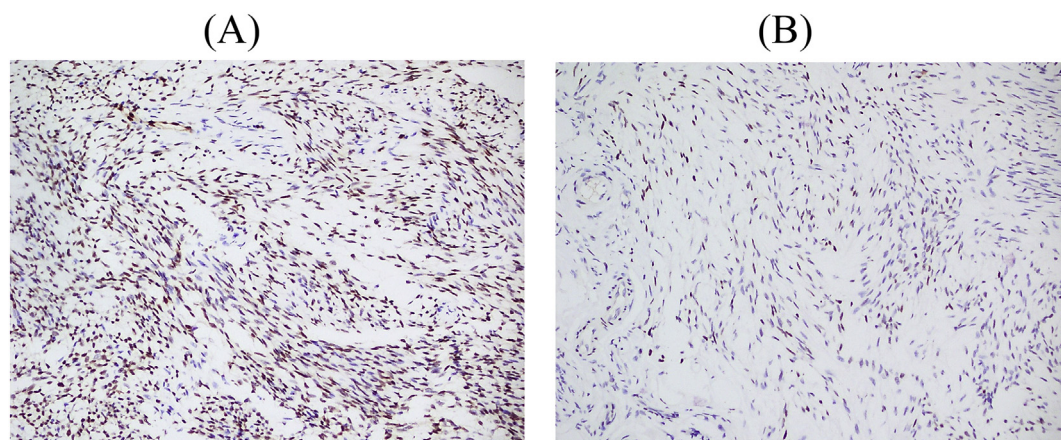


**Fig. 3.** Immunohistochemical features. A. Tumor cells showed diffuse nuclear staining for ERG. B. Focal and weak expression of SATB2.

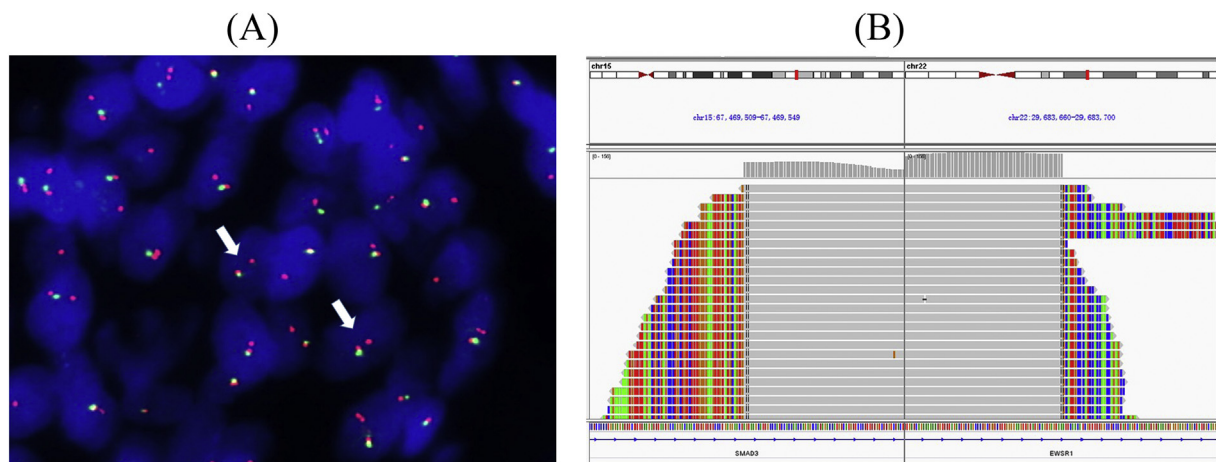


Fig. 4. Molecular detection. A. FISH assay showed unbalanced rearrangement of *EWSR1* gene. (B). NGS identified *EWSR1-SMAD3* fusion gene.

Table 1

Summary of clinical, immunohistochemical and molecular features of *EWSR1-SMAD3* positive fibroblastic tumor.

Authors	Age (yrs)/Sex	Location	Size (cm)	ERG (IHC)	FISH	NGS	Follow-up (mo)
Kao et al.	1/M	Left heel	1	+	Unbalanced rearrangement of SMAD3 and EWSR1	EWSR1-SMAD3	LR, 14
	61/F	Foot	2	+	EWSR1 gene rearrangement	EWSR1-SMAD3	NA
	58/F	Toe	1.1	+	EWSR1 gene rearrangement	EWSR1-SMAD3	LR, 5
Michal et al.	5/F	Hand	1.2	+	NA	EWSR1-SMAD3	LR, 120
	68/F	Thumb	1.5	+	NA	EWSR1-SMAD3	ANED
	39/F	Calf	1	+	NA	NA	ANED
	34/F	Left foot	1.1	+	Unbalanced rearrangement of EWSR1	EWSR1-SMAD3	Recent case
Zhao et al.(current case)	22/M	Right forefoot	1.3	+	Unbalanced rearrangement of EWSR1	EWSR1-SMAD3	LR, 24

ANED, alive without evidence of disease; IHC, immunohistochemistry; NA, not available; FISH, fluorescence in situ hybridization; NGS, next-generation sequencing.

often in juxta-articular locations. It is a spindle cell sarcoma showing variable epithelial differentiation and harboring specific *SS18-SSX* fusion gene. Calcifying aponeurotic fibroma also arises on the distal extremities and is characterized by fibromatosis-like infiltrative spindle cell component and scattered nodular calcified component which often has a chondroid appearance. The detection of the *FNI-EGF* gene fusion may be helpful for the distinction. *NTRK* rearranged spindle cell mesenchymal tumor is an emerging entity spanning a wide spectrum of morphologies and histologic grades (Davis et al., 2019), including the recently described lipofibromatosis-like neural tumor (Agaram et al., 2016). By immunohistochemistry, the majority of cases often show diffuse staining of pan-TRK, with frequent co-expression of S100 and CD34 in low grade tumors. All the lesions are characterized by *NTRK* rearrangement with various fusion partners. The paucicellular zones with collagenous or myxoid stroma may make *EWSR1-SMAD3* positive fibroblastic tumor resemble MPNST, however, the absence of S-100 protein and SOX10 immunoreactivity, and retained H3K27me3 expression do not favor a diagnosis of MPNST (Pekmezci et al., 2017). Phosphaturic mesenchymal tumor (PMT) is a rare but distinctive neoplasm that may cause tumor-induced osteomalacia. Histologically, it is composed of bland spindle cells characterized by producing “smudgy”-appearing matrix or “grungy” calcification. Of note, expression of ERG and SATB2 were also documented in PMT (Tajima et al., 2016; Agaimy et al., 2017), showing overlapping immunophenotypes with *EWSR1-SMAD3* positive fibroblastic tumor. However, PMT is molecularly characterized by *FNI-FGFR1* or *FNI-FGF1* fusion genes (Lee et al., 2016), which may help distinguishing PMT from *EWSR1-SMAD3* positive fibroblastic tumor.

In conclusion, our study further supported that *EWSR1-SMAD3* positive fibroblastic tumor represented a distinctive clinicopathologic entity. In challenging cases that lack a specific line of differentiation both morphologically and immunohistochemically, NGS analysis may be helpful for identifying novel unknown genetic aberrations, which

may be characteristic hallmarks of the lesions.

#### Declaration of Competing Interest

The authors state that there are no conflicts of interest with respect to the research, authorship, and/or publication of this article.

#### Acknowledgement

The authors would thank Origimed for assistance in NGS analysis.

#### References

- Agaimy, A., Michal, M., Chiosea, S., et al., 2017. Phosphaturic mesenchymal tumors: clinicopathologic, immunohistochemical and molecular analysis of 22 cases expanding their morphologic and immunophenotypic spectrum. *Am. J. Surg. Pathol.* 41 (10), 1371–1380.
- Agaram, N.P., et al., 2016. Recurrent *NTRK1* gene fusions define a novel subset of locally aggressive lipofibromatosis-like neural tumors. *Am. J. Surg. Pathol.* 40, 1407–1416.
- Buttner, C., Skupin, A., Rieber, E.P., 2004. Transcriptional activation of the type I collagen genes *COL1A1* and *COL1A2* in fibroblasts by interleukin-4: analysis of the functional collagen promoter sequences. *J. Cell. Physiol.* 198 (2), 248–258.
- Choi, E.Y., Thomas, D.G., McHugh, J.B., et al., 2013. Undifferentiated small round cell sarcoma with t(4;19)(q35;q13.1) *CIC-DUX4* fusion: a novel highly aggressive soft tissue tumor with distinctive histopathology. *Am. J. Surg. Pathol.* 37 (9), 1379–1386.
- Davis, J.L., Lockwood, C.M., Stohr, B., et al., 2019. Expanding the spectrum of pediatric *NTRK*-rearranged mesenchymal tumors. *Am. J. Surg. Pathol.* 43 (4), 435–445.
- Flanders, K.C., 2004. Smad3 as a mediator of the fibrotic response. *Int. J. Exp. Pathol.* 85 (2), 47–64.
- Groisberg, R., Roszik, J., Conley, A., et al., 2017. The role of next-generation sequencing in sarcomas: evolution from light microscope to molecular microscope. *Curr. Oncol. Rep.* 19 (12), 78.
- Houen, G., 2019. Commentary: Calreticulin - oncogene, anti-oncogene, or both? *Curr. Protein Pept. Sci.* 20 (1), 111–112.
- Kao, Y.C., Flucke, U., Eijkelenboom, A., et al., 2018. Novel *EWSR1-SMAD3* gene fusions in a group of acral fibroblastic spindle cell neoplasms. *Am. J. Surg. Pathol.* 42 (4), 522–528.
- Kolosova, I., Nethery, D., Kern, J.A., 2011. Role of Smad2/3 and p38 MAP kinase in TGF-beta1-induced epithelial-mesenchymal transition of pulmonary epithelial cells. *J.*

- Cell. Physiol. 2269 (5), 1248–1254.
- Lee, J.C., Su, S.Y., Changou, C.A., Yang, R.S., et al., 2016. Characterization of FN1-FGFR1 and novel FN1-FGF1 fusion genes in a large series of phosphaturic mesenchymal tumors. *Mod. Pathol.* 29 (11), 1335–1346.
- Liu, F., 2006. Smad3 phosphorylation by cyclin-dependent kinases. *Cytokine Growth Factor Rev.* 17, 9–17.
- Matsuura, I., et al., 2004. Cyclin-dependent kinases regulate the antiproliferative function of Smads. *Nature* 430, 226–231.
- Michal, M., Berry, R.S., Rubin, B.P., et al., 2018. EWSR1-SMAD3-rearranged fibroblastic tumor: an emerging entity in an increasingly more complex group of fibroblastic/myofibroblastic neoplasms. *Am. J. Surg. Pathol.* 42 (10), 1325–1333.
- Miettinen, M., Felisiak-Golabek, A., Luiña Contreras, A., et al., 2019. New fusion sarcomas: histopathology and clinical significance of selected entities. *Hum. Pathol.* 86, 57–65.
- Ooshima, A., Park, J., Kim, S.J., 2019. Phosphorylation status at Smad3 linker region modulates transforming growth factor-beta-induced epithelial-mesenchymal transition and cancer progression. *Cancer Sci.* 110 (2), 481–488.
- Pekmezci, M., Cuevas-Ocampo, A.K., Perry, A., Horvai, A.E., 2017. Significance of H3K27me3 loss in the diagnosis of malignant peripheral nerve sheath tumors. *Mod. Pathol.* 30 (12), 1710–1719.
- Pierron, G., Tirode, F., Lucchesi, C., et al., 2012. A new subtype of bone sarcoma defined by BCOR-CCNB3 gene fusion. *Nat. Genet.* 44 (4), 461–466.
- Tajima, S., Takashi, Y., Ito, N., et al., 2016. ERG and FLI1 are useful immunohistochemical markers in phosphaturic mesenchymal tumors. *Med. Mol. Morphol.* 49 (4), 203–209.
- Verrecchia, F., Chu, M.L., Mauviel, A., 2001. Identification of novel TGF-beta/Smad gene targets in dermal fibroblasts using a combined cDNA microarray/promoter transactivation approach. *J. Biol. Chem.* 276 (20), 17058–17062.
- Zawel, L., Dai, J.L., Buckhaults, P., et al., 1998. Human Smad3 and Smad4 are sequence-specific transcription activators. *Mol. Cell* 1 (14), 611–617.